Check for updates

How to cite: *Angew. Chem. Int. Ed.* **2024**, *63*, e202407424
doi.org/10.1002/anie.202407424

VIP **Supramolecular Chemistry** *Very Important Paper*

Fuel-Driven Dynamic Combinatorial Peptide Libraries

*Fabian Späth, Héctor Soria-Carrera, Michele Stasi, Judit Sastre, Brigitte A. K. Kriebisch, and Job Boekhoven**

Abstract: Dynamic combinatorial chemistry (DCC) creates libraries of molecules that are constantly interchanging in a dynamic combinatorial library. When a library member self-assembles, it can displace the equilibria, leading to emergent phenomena like its selection or even its replication. However, such dynamic combinatorial libraries typically operate in or close to equilibrium. This work introduces a new dynamic combinatorial chemistry fueled by a catalytic reaction cycle that forms transient, out-of-equilibrium peptide-based macrocycles. The products in this library exist out of equilibrium at the expense of fuel and are thus regulated by kinetics and thermodynamics. By creating a chemically fueled dynamic combinatorial library with the vast structural space of amino acids, we explored the liquid-liquid phase separation behavior of the library members. The study advances DCCs by showing that peptide structures can be engineered to control the dynamic library's behavior. The work paves the way for creating novel, tunable material systems that exhibit emergent behavior reminiscent of biological systems. These findings have implications for the development of new materials and for understanding life's chemistry.

Introduction

Molecules in dynamic combinatorial libraries react with one another reversibly to form a network of library members.[1] Such dynamic combinatorial chemistries generate a mixture of compounds that interconvert into one another. Processes like self-assembly,[2] folding,[3] or hybridization can displace the equilibria, leading to emergent phenomena like replication.[4] Various dynamic covalent bonds have been explored to create dynamic combinatorial libraries, including metathesis,[5] hydrazone formation,[6] disulfide exchange,[7] peptide bond formation,[8] or transamination.[9] Such dynamic combinatorial libraries serve as a great model for the cellular reaction networks, which are also dynamic combinatorial libraries. For example, building blocks like nucleotides or amino acids form a vast library of oligonucleotides and proteins. Complex replication and translation machinery based on enzymes tightly regulate the product distribution in such networks in energy-consuming processes. When such reaction networks exist out of equilibrium, the abundance of library members is no longer solely controlled by thermodynamics but also by kinetics.

As a model for biology's complex, out-of-equilibrium reaction networks, dynamic combinatorial libraries out of equilibrium have been designed.[10] For example, in dissipative dynamic libraries, catalytic reaction cycles that convert reagents with high chemical potential (fuels) into products with low chemical potential (wastes) generate dynamic libraries that can only be at the expense of chemical potential. Specifically, fuel conversion into waste is required to form a dynamic covalent bond between library members of the combinatorial library. A backward reaction breaks the bonds between the library members. The combination of fuel-driven bond formation and spontaneous bond cleavage means that dynamic covalent bonds are present, and library members can only exist when fuel is supplied. After the conversion of the fuel, the library will collapse towards equilibrium. For example, Otto described recently self-assembling self-replicators based on disulfide exchange that require an oxidizing agent as fuel to form but are reacted back by reducing agents of the environment. The ability of a product to assemble catalyzed the formation of its building blocks, thereby shifting the concentrations away from the equilibrium conditions.[11] Our group introduced transient anhydride linkages between isophthalic acid building blocks. In this system, the self-assembly[12] and hybridization of oligomers[13] also influenced the reaction kinetics by increasing the activation and decreasing the hydrolysis rates of certain library members.

The scope of chemically fueled dynamic combinatorial libraries remains limited. Peptide-based building blocks can help to broaden the scope of such systems by the large variety of structures and straightforward preparation.[14] Thus, in this work, we combine the power of chemically fueled dynamic combinatorial libraries with the vast library space of amino acids. We demonstrate how molecular design affects the outcome of the library and resulting self-assembled structures.

[*] F. Späth, H. Soria-Carrera, M. Stasi, J. Sastre, B. A. K. Kriebisch, J. Boekhoven
School of Natural Sciences, Department of Bioscience, Technical University of Munich
Lichtenbergstrasse 4, 85748 Garching (Germany)
E-mail: job.boekhoven@tum.de

© 2024 The Author(s). Angewandte Chemie International Edition published by Wiley-VCH GmbH. This is an open access article under the terms of the Creative Commons Attribution Non-Commercial License, which permits use, distribution and reproduction in any medium, provided the original work is properly cited and is not used for commercial purposes.

© 2024 The Author(s). Angewandte Chemie International Edition published by Wiley-VCH GmbH

Results and Discussion

Molecular Design Affects the Library Products

For a dynamic combinatorial library based on carboxylate activation via carbodiimides, we require building blocks with two functional groups that can dimerize through a dynamic covalent bond. Moreover, the product dimer should again be a library member, such that it can form a trimer. Thus, a building block needs to be bi-functional—it should contain both the donating and receiving components for the dynamic covalent bond (Scheme 1A). Finally, to create a dynamic combinatorial library under kinetic control, the building blocks should be coupled to a reaction cycle. The building blocks should be the thermodynamically favored state. In contrast, the library's products exist only higher in the free energy landscape. Put differently, the dynamic covalent bond should be formed upon reacting with a high-energy fuel and spontaneously decaying to the building block state.

We chose as a chemically fueled, dynamic covalent bond an ester between a peptide's C-terminus and a tyrosine's phenol. In aqueous media, an ester will not form spontaneously but requires an activating agent (fuel-driven activation). Moreover, it will hydrolyze spontaneously (deactivation). Specifically, we work with the peptide motif Ac-X-Y-X-X-D-OH, in which Y stands for tyrosine and carries the phenol side group, D means aspartic acid, and X being either glycine, arginine, alanine, phenylalanine or tryptophan to direct the self-assembly of the peptides (Scheme 1B). In previous work, we have demonstrated that C-terminal aspartic acid easily converts into its corresponding anhydride by reaction with carbodiimides like EDC. EDC first activates one carboxylate, and the O-acylurea is converted by an intramolecular attack of the second carboxylate group to an anhydride. The anhydride is hydrolytically unstable and has a limited lifetime in aqueous media.[15] Depending on the structure of the starting material, transient vesicles,[16] fibers,[17] or complex coacervate-based[18] and oil-based droplets[19] were accessible with this chemical reaction cycle. We hypothesized that a tyrosine's phenol as a nucleophile would react with such anhydrides to form an intermolecular phenol ester. The resulting ester contains a C-terminal aspartic acid and a free tyrosine and can thus continue the process. Put differently, a monomer can react with fuel to be dimerized, after which it can further react to make trimers and further oligomers. Besides, all peptides can also form intramolecular esters corresponding to the cyclic monomer, cyclic dimer, and further cyclic oligomers. Since we anticipated the potential formation of cyclized products by this chemistry, we reduced the backbone flexibility, thereby restricting the cyclization pathways. Finally, because of the hydrolytically labile nature of phenol esters,[20] all library members are transient and will decay to their monomer state unless constantly supplied with fuel. We emphasize that with this design, every product that has hydrolyzed back to its initial state can form the other products again after activation as long as fuel is still present. However, due to the significant differences in the time scales between product formation and ester hydrolysis, this process is relatively slow compared to some dynamic combinatorial libraries under equilibrium control.

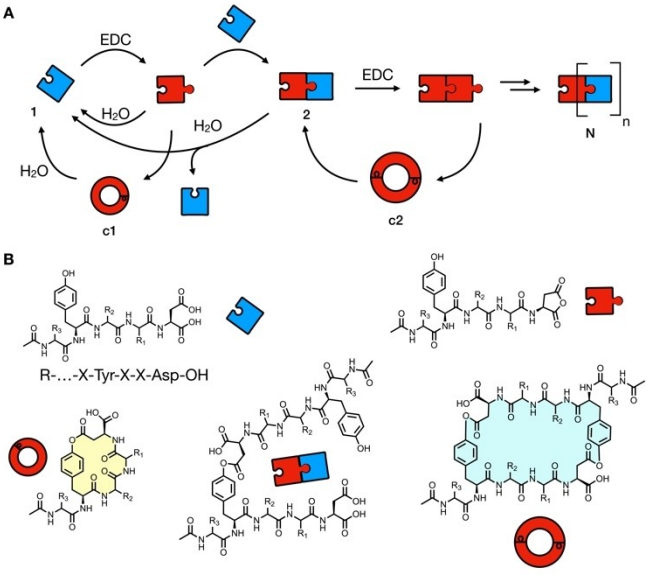

Scheme 1. A. Schematic representation of a dynamic combinatorial library built from a bifunctional precursor. The depicted cycle also includes cyclization pathways, forming an intramolecular cyclic monomer and an intermolecular cyclic dimer. **B**. Schematic representation of the peptide core structure Ac-X-Y-X-X-D-OH fueled with the carbodiimide fuel EDC. Selected products are shown.

We tested the simplest library member possible, Ac-YGGD-OH, in which G stands for glycine, the smallest natural amino acid (Figure 1). We used 3 mM of peptide in 200 mM MES at pH 5.3. We applied 10 mM of the chemical fuel and, after 45 minutes, analyzed the outcome of the chemical reaction cycle using HPLC (Figure 1B). Excitingly, we observed around 15 new peaks in the chromatogram, demonstrating that the dynamic combinatorial library produces an abundance of new species. By mass spectrometry, we identified the molecular weights corresponding to the cyclic monomer, linear dimer, cyclic dimer, and linear trimer (see SI for details). Noteworthy, potential isomers with the same molecular weight exist in this dynamic combinatorial library. For example, a linear trimer has the same molecular weight as a branched dimer, while a cyclic trimer has the same molecular weight as a cyclic dimer with a branch. This combinatorial explosion explains the high number of product peaks in a chromatogram. Nevertheless, these new species were hydrolyzing over time, and after roughly 15 hours, the last peak had completely decayed. The decay of all peaks implies that all the new library members formed in response to fuel were transient.

To control the formation of the library members, we substituted the flexible glycine for a non-nucleophilic, cationic amino acid. We hypothesized that this amino acid can form a salt bridge with the C-terminal aspartic acid, facilitating peptide cyclization. Indeed, when comparing the chromatograms of Ac-YGGD-OH and Ac-YRGD-OH 45 minutes after adding EDC, two main products were favored

© 2024 The Author(s). Angewandte Chemie International Edition published by Wiley-VCH GmbH

15213773, 2024, 42, Downloaded from https://onlinelibrary.wiley.com/doi/10.1002/anie.202407424, Wiley Online Library on [14/11/2024]. See the Terms and Conditions (https://onlinelibrary.wiley.com/terms-and-conditions) on Wiley Online Library for rules of use; OA articles are governed by the applicable Creative Commons License

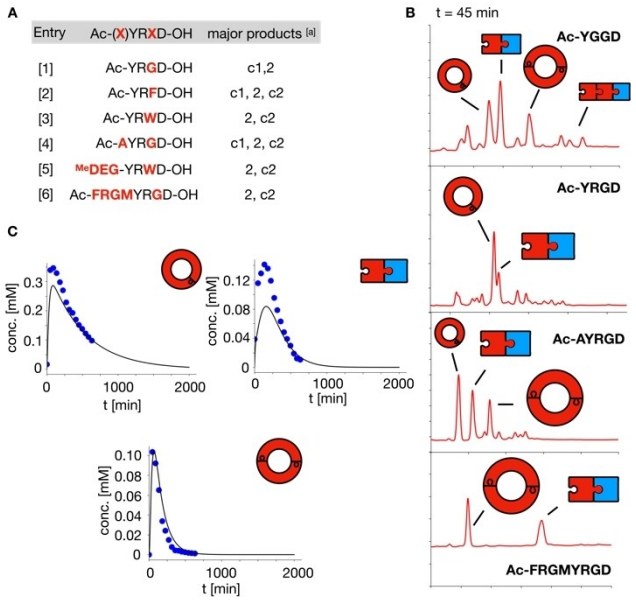

Figure 1. **The peptide library and their main products after fueling with EDC. A.** The main products were determined as the transient products with the highest intensity in the chromatograms and those that could be identified unambiguously. The cyclodimer product was differentiated from the cyclic monomer by isolating the product and hydrolyzing it after readjusting the pH to 5.3. The evolution of the transient products during the hydrolysis was monitored by HPLC. **B.** Comparison of the different chromatograms of the dynamic combinatorial libraries with different peptides 45 minutes after adding EDC. **C**. The kinetic profiles when 3 mM Ac-AYRGD-OH was fueled with 10 mM of EDC. The markers represent HPLC data, and the solid line is the kinetic model data.

in the case of Ac-YRGD-OH, namely the cyclic monomer and a smaller fraction of linear dimer (Figure 1B). To substantiate the idea of pre-organization, we also analyzed the evolution of products from Ac-YRGD-OH in the presence of 1.9 M guanidinium chloride, which is known to disrupt salt bridges.[21] In the experiment, the yield of cyclic monomer and dimer products decreased by 42% (SI Figure 5). Additionally, we found that solutions of MES buffer with or without 3 mM of Ac-YRGD-OH in MES buffer at pH 5.3 had similar scattering rate by dynamic light scattering which helped to rule out any pre-aggregation of the peptide.

To further control the outcome of the combinatorial library, we introduced bulky amino acids besides the arginine. Specifically, we substituted the remaining glycine for phenylalanine or tryptophan (Ac-YRFD-OH or Ac-YRWD-OH). Moreover, we also prepared a peptide with an acetyl-protected alanine at the N-terminus (Ac-AYRGD-OH). In line with the literature,[22] we hypothesized that the increased bulkiness diminishes cyclic monomer formation, favoring dimerization and cyclic dimer formation. After the fuel was applied, we observed that the ratio of cyclic monomer to linear dimer and cyclic dimer had decreased. Consequently, there were now only three main products in the chromatograms – cyclic monomer, dimer, and cyclic dimer. Moreover, in the case of Ac-YRWD-OH, hardly any cyclic monomer was formed. Comparing the total amount of products to the starting material showed that the arginine-containing peptides, compared to Ac-YGGD-OH, form up to 50% more ester products, further showing the preorganization effect. When we further modified the N-termini with peptides, we found that the general trend still held, *i.e.*, the main products were dimer and cyclic dimer (Figure 1A). These modifications allowed us, in later stages of the work, to control the self-assembly of the products of this combinatorial library.

With the peptide Ac-AYRGD-OH, we followed the kinetics of the reaction cycle in more detail by HPLC (Figure 1C). After adding 10 mM of EDC as fuel to 3 mM of peptide, we found that the EDC was consumed within 2 hours. The consumption of EDC produced three major new peaks that we attributed to the cyclic monomer, regular dimer, and cyclodimer. Each of these peaks, as well as the smaller peaks, were transient and had completely disappeared after 6 hours. We did not find a peak for the corresponding O-acylisourea or the aspartic acid anhydrides, most likely because they are converted quickly into esters. An HPLC analysis further showed that the ratio of peptide to the fuel EDC changes the relative amount of the individual products formed. At a high peptide-to-EDC ratio, e.g., 10 mM of peptide fueled with 20 mM EDC, a larger relative amount of dimer product and a lower amount of cyclomonomer is formed after 90 min (c1:2:c2 of 2.5:4.7:1) compared to 1 mM of peptide that was fueled with 10 mM of EDC (10:1:1) (Supporting Figure 1). Furthermore, for Ac-YRGD-OH and Ac-AYRGD-OH, we tested the influence of the time points of guanidinium chloride addition to the reaction mixture. The experiments showed that the earlier the time point when guanidinium chloride was added to the cycle, the greater the inhibition of product formation was (Supporting Figure 6). Both observations nicely show how the system responds dynamically to the conditions.

Using the kinetic profiles, we developed a kinetic model that predicts the evolution of the reaction cycle by fitting the HPLC data using a set of differential equations for each reaction. The reactions we consider are the peptide anhydride formation, and the peptide anhydride can react further inter- or intramolecularly with tyrosine to form a cyclic monomer or linear dimer. The linear dimer can also form its respective anhydride, which can again react intramolecularly to the cyclic dimer. We did not consider reactions further to the linear trimer as it was only observed in neglectable amounts or not at all. Hydrolysis can revert these reactions, but interestingly, the different ester products showed different hydrolysis rates that could be extracted graphically (5.77 h, 1.92 h, and 1.44 for the cyclomonomer, linear dimer, and cyclodimer, respectively) (see Supporting Information for details). We also investigated possible reaction pathways further by testing for transesterification. Specifically, we isolated the cyclomonomer product of Ac-AYRGD-OH and added unreacted peptide. Since we did not observe the formation of the linear dimer, we exclude potential transesterification from the list of possible reaction pathways, at least starting from the cyclomonomer product (Supporting Figure 7). However, it is obvious that other transesterification pathways of products with different reactivity, e.g.,

© 2024 The Author(s). Angewandte Chemie International Edition published by Wiley-VCH GmbH

15213773, 2024, 42, Downloaded from https://onlinelibrary.wiley.com/doi/10.1002/anie.202407424, Wiley Online Library on [14/11/2024]. See the Terms and Conditions (https://onlinelibrary.wiley.com/terms-and-conditions) on Wiley Online Library for rules of use; OA articles are governed by the applicable Creative Commons License

linear products, cannot be completely ruled out. Overall, our kinetic model shows good agreement with the concentration traces of the individual species that were obtained from HPLC, further substantiating our proposed reaction cycle.

Overall, our proposed peptide family generates a new chemically fueled dynamic combinatorial library. The peptide's substitution pattern structure drastically affects the dynamic, transient library.

Fueled Phase Separation by Simple Coacervation

Next, we tested whether certain library members could assemble or phase separate. Short peptide sequences with multiple aromatic residues have been shown to phase separate into simple coacervate-based droplets, *i.e.*, droplets with a high water content formed by a self-interacting building block.[23] Even cationic sequences as short as dipeptides with aromatic residues could assemble into such droplets.[24] Since cation-π interactions are one of the main driving forces for such phase-separations of peptides,[25] we hypothesized that the ester products derived from Ac-YWRD-OH could also phase-separate upon fueling the peptide with the right amount of EDC.

After fueling the peptide Ac-YRWD-OH with EDC (3 mM EDC added to 10 mM peptide or 10 mM EDC added to 20 mM peptide), the sample rapidly turned turbid, indicative of the formation of assemblies sufficiently large to scatter light (Figure 2A). Noteworthy, the peptide Ac-YRFD-OH did not show any sign of self-assembly under the same fueling conditions likely due to weaker cation-π interactions between arginine and phenylalanine compared to tryptophan or stronger hydrophobic interactions.[26] The turbidity evolution was tracked by UV-Vis spectroscopy with a plate reader at a wavelength of 600 nm (Figure 2A). The influence of intermolecular interaction between arginine and tryptophans on self-assembly was further investigated by comparing the effects of NaCl and guanidinium chloride. Guanidinium chloride completely prevented self-assembly, whereas NaCl had no notable effect (Supporting Figure 8). The turbidity emerged and decayed after 10 hours when 10 mM peptide was fueled with 20 mM of EDC. Laser scanning confocal microscopy revealed the increased turbidity resulted from small amorphous assemblies (Figure 2B).

We tested the composition of the assemblies by spinning down the samples 90 minutes after fuel addition. We then analyzed the supernatant by HPLC and used these concentrations as a reference for components that did not assemble. We analyzed the composition of samples that had not been spun down, but instead, we dissolved all the assemblies by diluting the solution with 4M guanidinium chloride solution and rigorous mixing. We found that the assemblies were a co-assembly of peptide precursor, linear dimer, and cyclodimer product. To put that into the context of the dynamic combinatorial library members, 54% of the total linear dimer was in the assembly, whereas the rest remained in the solution. In contrast, 69% of the total cyclodimer concentration is taken up in the assemblies,

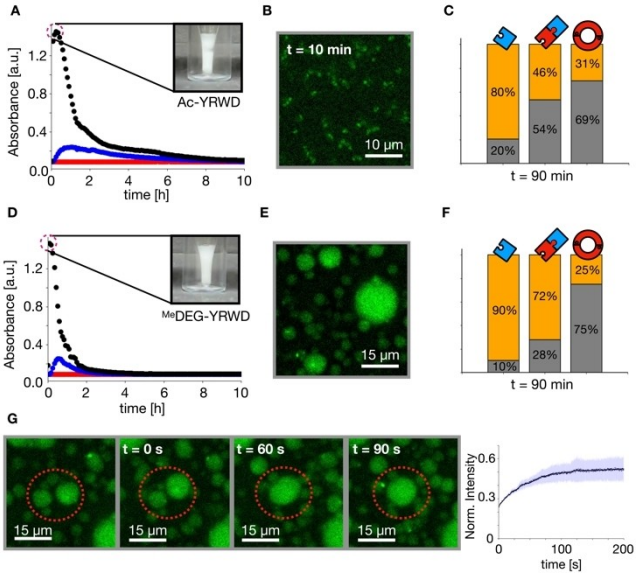

Figure 2. **Chemically fueled assembly of the X-YRWD-OH family. A.** Evolution of turbidity of Ac-YRWD-OH assemblies at different concentrations and different amounts of EDC (black: 10 mM peptide and 20 mM EDC, blue: 3 mM peptide and 10 mM EDC, red: 1 mM peptide and 10 mM EDC). **B.** Confocal micrographs 10 mM Ac-YWRD-OH fueled with 20 mM EDC in 200 mM MES buffer at pH 5.3. NBD-G(RG)$_2$N-NH$_2$ was used as a fluorescent dye. **C.** Distribution of total concentrations of the peptide monomer, linear dimer, and cyclodimer species (grey: in droplets, orange: in the supernatant) as determined by HPLC (see Supporting Information and Methods for details). **D.** Turbidity evolution of 2-[2-(2-methoxyethoxy)ethoxy]acetyl-YRWD-OH under different conditions (black: 10 mM peptide and 20 mM EDC, blue: 3 mM peptide and 10 mM EDC, red: 1 mM peptide and 10 mM EDC). **E.** Confocal microscopy image of a sample of 10 mM peptide fueled with 20 mM of EDC in 200 mM MES buffer at pH 5.3. NBD-G(RG)$_2$N-NH$_2$ was used as a fluorescent dye. **F.** Distribution of the total concentration of peptide monomer, linear dimer, and cyclodimer species (grey: in droplets, orange: in the supernatant) as determined by HPLC **G.** Left: Confocal micrographs of liquid droplets from 10 mM peptide fueled with 20 mM EDC, 10 minutes after EDC addition. Right: Fluorescence recovery from FRAP analysis.

indicating that the cyclodimer has a higher tendency to self-assemble (Figure 2C).

As we aimed for liquid assemblies through phase separation, we modified the YRWD-OH peptide sequence. We added a 2-[2-(2-methoxyethoxy)ethoxy]acetic acid tail to the N-terminus of the peptide structure to increase its overall solubility without influencing the reactive core. This peptide also showed a fast increase in turbidity upon fueling with EDC (Figure 2D). Confocal microscopy revealed micron-sized spherical assemblies that rapidly fused, from which we concluded they were liquid (Figure 2E). Spinning down the droplets and analyzing the supernatant revealed that most cyclic dimer partitions into these droplets (75%) (Figure 2F). The liquid nature of the simple coacervate droplets was further investigated by FRAP analysis, which revealed a fast recovery of fluorescence intensity after bleaching (Figure 2G). The corresponding diffusion coefficient was determined to D = 0.063 $\mu m^2 \cdot s^{-1}$. Finally, We determined the water content of the simple coacervates and

© 2024 The Author(s). Angewandte Chemie International Edition published by Wiley-VCH GmbH

15213773, 2024, 42, Downloaded from https://onlinelibrary.wiley.com/doi/10.1002/anie.202407424, Wiley Online Library on [14/11/2024]. See the Terms and Conditions (https://onlinelibrary.wiley.com/terms-and-conditions) on Wiley Online Library for rules of use; OA articles are governed by the applicable Creative Commons License

assigned them to 89.5% for Ac-YRWD-OH and 59.5% for ^{Me}DEG-YRWD-OH (see Supporting Information Methods Section). This also showed that the higher fluidity is indeed a consequence of the differences in the molecular design and not the water contents, as both phases are highly hydrated.

Fueled Phase Separation by Complex Coacervation

Complex coacervation describes the phase separation of at least two charged components, usually involving a polyionic species. We reasoned that combining our in-situ generated cationic building blocks with polyanions enabled us to create droplets through complex coacervation. Given the chemically fueled nature of our chemically fueled dynamic combinatorial library, complex coacervation of the library members should lead to active droplets, *i.e.*, those requiring fuel to be sustained. We first tested the peptide structure Ac-FRGMYRGD-OH in combination with the polyanion PSS (poly(styrene sulfonate)) because it forms large amounts of linear dimer and cyclodimer products in response to EDC (Figure 1B). Besides, the peptide is zwitterionic (+2, -2) and overall charge neutral. In contrast, the linear dimer has an overall charge of +1, and the cyclodimer has an overall charge of +2. In other words, we expect minimal interaction between the peptide and polyanions. In contrast, the products of the reaction cycle are expected to interact strongly with the polyanion to form complex coacervate-based droplets. This chemically fueled charge switching has been previously explored in active droplets but not in the context of a dynamic combinatorial library.[18, 27] To further enhance the interaction with polyanions, we added methionine (M), known for its interactions with π-systems, thus driving phase separation.[28]

Indeed, when we combined 10 mM peptide with 20 mM EDC in 200 mM MES buffer at pH 5.3 in the presence of 1 mM polyanion PSS, turbidity quickly emerged. The turbidity peaked around 1 hour after fuel addition and slowly declined over 24 hours when the absorbance value reached its initial value again (Figure 3A). We tested the coacervate composition by spinning down the droplets and analyzing the supernatant. After 90 minutes, the EDC was fully consumed, and we found that 31% of the total cyclodimer was taken up into the droplets together with 15 % of the linear dimer. We could further determine the water content of the complex coacervates to 65% on average (see Supporting Information Methods Section). After 450 minutes, no more peptide precursor is present in the coacervate droplets, and 20% of the linear dimer and 38% of the total cyclodimer concentration in the mixture are concentrated in the coacervate droplets. These results show that the cyclodimer is the most potent coacervating agent among the library members (Figure 3B). Similar mixtures without PSS did not show any evidence of assemblies, from which we conclude that the assemblies are a complex coacervate between peptide and PSS.

We further studied the assemblies by confocal microscopy and found micron-sized droplets that rapidly fused,

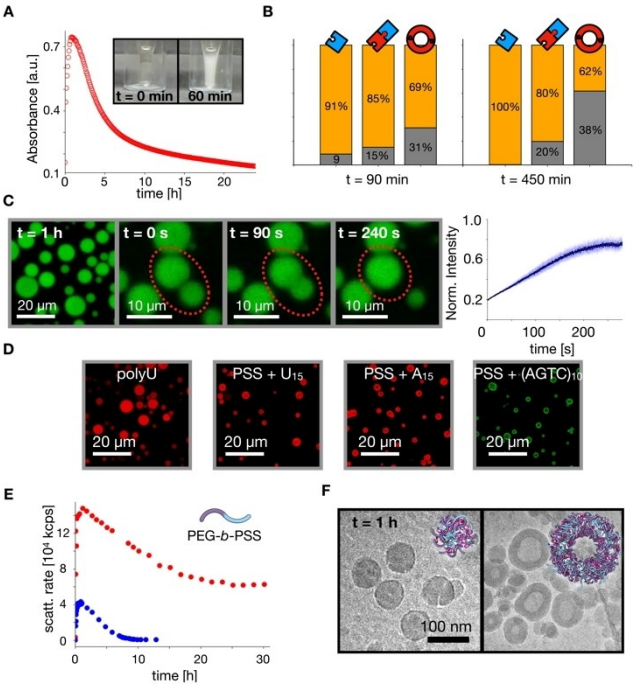

Figure 3. **Complex coacervation of Ac-FRGMYRGD-OH with the polyanion poly(styrene sulfonate) – PSS. A**. Evolution of turbidity of a sample consisting of 10 mM of peptide that was fueled with 20 mM of EDC in the presence of 1 mM of PSS (expressed in monomer concentration). **B**. The different concentrations of the peptide precursor, linear dimer, and cyclodimer of the peptide in the coacervate phase (grey) and in the supernatant (orange) at different time points in the cycle. **C**. Confocal microscopy images of the coacervate droplets with NBD-G(RG)$_2$N-NH$_2$ as the fluorescent dye. 10 mM of peptide were fueled with 20 mM EDC in the presence of 1 mM PSS, all in 200 mM MES buffer at pH 5.3. The coacervate droplets fuse and show fluorescence recovery in FRAP analysis. **D**. Confocal laser micrographs of oligonucleotide and mixed PSS-oligonucleotide coacervates (10 mM of Ac-FRGMYRGD-OH with 20 mM of EDC in the presence of 1 mM polyanion expressed in monomer units). Left: 1 mM of polyU as the polyanion with 200 nM of Cy5-U$_{15}$. Other samples: 1 mM PSS with 200 nM of Cy5-U$_{15}$, Cy5-A$_{15}$ or Cy3-(AGTC)$_{10}$ (from left to right). All images were taken one hour after the EDC was added. **E**. DLS analysis of coacervate core micelles from the peptide with EDC in the presence of 1 mM of the block copolymer PEG$_{5K}$-b-PSS$_{77}$. Red trace: 10 mM of peptide fueled with 20 mM of EDC. Blue trace: 3 mM of the peptide fueled with 10 mM of EDC in 200 mM MES at pH 5.3. **F**. Cryo-TEM images of coacervate core micelles one hour after adding 20 mM EDC to 10 mM of peptide and 1 mM of the block copolymer (expressed in charge concentrations).

from which we concluded they were liquid (Figure 3C). Furthermore, FRAP experiments revealed fast fluorescence recovery with a diffusion coefficient (D) of 0.0145 μm^2·s^{-1}. To test whether the PSS-based coacervates were able to take up functional oligonucleotides, we combined them with the RNA-oligonucleotides Cy5-U$_{15}$ or Cy5-A$_{15}$, or the DNA-oligomer Cy3-(AGTC)$_{10}$. In all cases, the oligonucleotides were taken up into the coacervates but were more concentrated on the periphery of the droplets, suggesting a demixing tendency of the two polyanions. Aside from that, the coacervates were significantly smaller than those made from pure PSS (Figure 3D).

© 2024 The Author(s). Angewandte Chemie International Edition published by Wiley-VCH GmbH

15213773, 2024, 42, Downloaded from https://onlinelibrary.wiley.com/doi/10.1002/anie.202407424, Wiley Online Library on [14/11/2024]. See the Terms and Conditions (https://onlinelibrary.wiley.com/terms-and-conditions) on Wiley Online Library for rules of use; OA articles are governed by the applicable Creative Commons License

To test the peptide's versatility in making coacervates, we tested it with other anionic (block co-) polymers. First, we analyzed it in combination with 1 mM polyU as polyanion. The sample transiently turned turbid with EDC, similar to using PSS as polyanion (Supporting Figure 9). These polyU-based coacervates appeared as spherical droplets slightly smaller than the corresponding PSS-based coacervates (Figure 3D). It should be noted that the complex coacervate formation with both types of polyanions is highly responsive to the pH value of the solution. At pH 5, the turbidity cycles for both polyanions were shorter compared to pH 5.3, and they reach their maximum turbidity value later, whereas for pH 7, the solution did not fully revert to its initial transparency and precipitates are formed (Supporting Figure 10).

Next, we combined the peptide with block copolymers made from PEG and PSS to further tune their properties, *i.e.*, change their size. To test its ability to form complex coacervate core micelles (C3Ms), we applied 20 mM EDC to 10 mM of peptide in the presence of 1 mM of PEG_{5K}-b-PSS_{77} and monitored the assembly process by DLS (Figure 3E). This analysis showed a quick increase in scattering rate after EDC was added, indicating the immediate complexation of block copolymer by the dynamic combinatorial library members. The maximum scattering rate was reached after 1 hour, coinciding with the maximum turbidity for the complex coacervation of PSS homopolymer. Cryo-TEM further corroborated the formation of block copolymer assemblies upon fueling (Figure 3F). Specifically, the micrographs show large compound micelles of 80 to 100 nm diameter that coexist with polymersomes with a diameter around 150 nm. These sizes matched well with the z-average size obtained from DLS (Supporting Figure 11). The lifetime of the assemblies could be increased by adding more peptides and EDC (Figure 3E).

Conclusion

We found a new, versatile, dynamic covalent bond that exists only out of equilibrium at the expense of chemical energy. The tyrosine ester-based dynamic covalent bond creates a dynamic combinatorial library by expanding a chemical reaction cycle based on EDC and aspartic acid-derived peptides with an esterification pathway. We found the new bond gives rise to a dynamic mixture of cyclic and linear tyrosine esters that form intra- and intermolecularly. The kinetics of the chemical reactions are quantitatively understood, allowing us to tune the product distribution through molecular design. Moreover, we showed that, through molecular design, the library could be linked to simple or complex coacervation. We envision the resulting coacervates or coacervate core micelles with lifetimes of multiple hours could be attractive for future applications, e.g., for controlled release systems for DNA or RNA. They are also valuable models for membraneless organelles, which are also coacervate-based droplets regulated through chemical reaction cycles. Finally, we envisage these droplets as a powerful protocell model or a compartment in life's de novo synthesis.

Supporting Information

The authors have cited additional references within the Supporting Information.[27a, 29]

Acknowledgements

The BoekhovenLab is grateful for support from the TUM Innovation Network - RISE funded through the Excellence Strategy and the European Research Council (ERC starting grant 852187). This research was conducted within the Max Planck School Matter to Life, supported by the German Federal Ministry of Education and Research (BMBF) in collaboration with the Max Planck Society. F.S. is grateful for funding from the Deutsche Forschungsgemeinschaft via the International Research Training Group ATUMS (IRTG 2022). H.S.-C thanks the Alexander von Humboldt Foundation for a postdoctoral research fellowship. We thank Florian Leiß-Maier (TUM) for the assistance with LC-MS analysis. Open Access funding enabled and organized by Projekt DEAL.

Conflict of Interest

The authors declare no conflict of interest.

Keywords: Dynamic combinatorial library · Chemical reaction cycle · Complex coacervation · Simple coacervation · Liquid-liquid phase separation

[1] J. M. Lehn, A. V. Eliseev, *Science* **2001**, *291*, 2331–2332.
[2] a) B. Liu, M. A. Beatty, C. G. Pappas, K. Liu, J. Ottele, S. Otto, *Angew. Chem. Int. Ed.* **2021**, *60*, 13569–13573; b) Y. Cao, J. Yang, D. Eichin, F. Zhao, D. Qi, L. Kahari, C. Jia, M. Peurla, J. M. Rosenholm, Z. Zhao, S. Jalkanen, J. Li, *Angew. Chem. Int. Ed.* **2021**, *60*, 3062–3070; c) C. B. Minkenberg, F. Li, P. van Rijn, L. Florusse, J. Boekhoven, M. C. Stuart, G. J. Koper, R. Eelkema, J. H. van Esch, *Angew. Chem. Int. Ed.* **2011**, *50*, 3421–3424.
[3] a) B. Liu, C. G. Pappas, E. Zangrando, N. Demitri, P. J. Chmielewski, S. Otto, *J. Am. Chem. Soc.* **2019**, *141*, 1685–1689; b) C. G. Pappas, B. Liu, I. Maric, J. Ottele, A. Kiani, M. L. van der Klok, P. R. Onck, S. Otto, *J. Am. Chem. Soc.* **2021**, *143*, 7388–7393.
[4] a) J. M. Carnall, C. A. Waudby, A. M. Belenguer, M. C. Stuart, J. J. Peyralans, S. Otto, *Science* **2010**, *327*, 1502–1506; b) J. Li, P. Nowak, S. Otto, *J. Am. Chem. Soc.* **2013**, *135*, 9222–9239.
[5] a) J. A. Berrocal, M. M. Nieuwenhuizen, L. Mandolini, E. W. Meijer, S. Di Stefano, *Org. Biomol. Chem.* **2014**, *12*, 6167–6174; b) A. Kravchenko, B. J. J. Timmer, A. K. Inge, M. Biedermann, O. Ramström, *ChemCatChem* **2021**, *13*, 4841–4847; c) I. Colomer, A. Borissov, S. P. Fletcher, *Nat. Commun.* **2020**, *11*, 176.
[6] a) S. Kulchat, M. N. Chaur, J. M. Lehn, *Chemistry* **2017**, *23*, 11108–11118; b) J. Boekhoven, J. M. Poolman, C. Maity, F. Li,

© 2024 The Author(s). Angewandte Chemie International Edition published by Wiley-VCH GmbH

15213773, 2024, 42, Downloaded from https://onlinelibrary.wiley.com/doi/10.1002/anie.202407424, Wiley Online Library on [14/11/2024]. See the Terms and Conditions (https://onlinelibrary.wiley.com/terms-and-conditions) on Wiley Online Library for rules of use; OA articles are governed by the applicable Creative Commons License

L. van der Mee, C. B. Minkenberg, E. Mendes, J. H. van Esch, R. Eelkema, *Nat. Chem.* **2013**, *5*, 433–437.
[7] a) B. M. Matysiak, P. Nowak, I. Cvrtila, C. G. Pappas, B. Liu, D. Komaromy, S. Otto, *J. Am. Chem. Soc.* **2017**, *139*, 6744–6751; b) S. Otto, S. Kubik, *J. Am. Chem. Soc.* **2003**, *125*, 7804–7805.
[8] C. G. Pappas, R. Shafi, I. R. Sasselli, H. Siccardi, T. Wang, V. Narang, R. Abzalimov, N. Wijerathne, R. V. Ulijn, *Nat. Nanotechnol.* **2016**, *11*, 960–967.
[9] a) F. Schaufelberger, L. Hu, O. Ramstrom, *Chemistry* **2015**, *21*, 9776–9783; b) M. Ciaccia, S. Pilati, R. Cacciapaglia, L. Mandolini, S. Di Stefano, *Org. Biomol. Chem.* **2014**, *12*, 3282–3287.
[10] D. Del Giudice, E. Spatola, M. Valentini, G. Ercolani, S. Di Stefano, *ChemSystemsChem* **2022**, *4*.
[11] S. Yang, G. Schaeffer, E. Mattia, O. Markovitch, K. Liu, A. S. Hussain, J. Ottele, A. Sood, S. Otto, *Angew. Chem. Int. Ed.* **2021**, *60*, 11344–11349.
[12] C. M. E. Kriebisch, A. M. Bergmann, J. Boekhoven, *J. Am. Chem. Soc.* **2021**, *143*, 7719–7725.
[13] C. M. E. Kriebisch, L. Burger, O. Zozulia, M. Stasi, A. Floroni, D. Braun, U. Gerland, J. Boekhoven, *Nat. Chem.* **2024**, *16*, 1240–1249 .
[14] M. Tena-Solsona, J. Boekhoven, *Israel J. Chem.* **2019**, *59*, 898–905.
[15] M. Tena-Solsona, B. Riess, R. K. Grötsch, F. C. Lohrer, C. Wanzke, B. Kasdorf, A. R. Bausch, P. Müller-Buschbaum, O. Lieleg, J. Boekhoven, *Nat. Commun.* **2017**, *8*, 15895.
[16] C. Wanzke, A. Jussupow, F. Kohler, H. Dietz, V. R. I. Kaila, J. Boekhoven, *ChemSystemsChem* **2019**, *2*.
[17] B. A. K. Kriebisch, A. Jussupow, A. M. Bergmann, F. Kohler, H. Dietz, V. R. I. Kaila, J. Boekhoven, *J. Am. Chem. Soc.* **2020**, *142*, 20837–20844.
[18] C. Donau, F. Späth, M. Sosson, B. A. K. Kriebisch, F. Schnitter, M. Tena-Solsona, H. S. Kang, E. Salibi, M. Sattler, H. Mutschler, J. Boekhoven, *Nat. Commun.* **2020**, *11*, 5167.
[19] L. Tebcharani, C. Wanzke, T. M. Lutz, J. Rodon-Fores, O. Lieleg, J. Boekhoven, *J. Control. Release* **2021**, *339*, 498–505.
[20] D. Gimenez, A. Phelan, C. D. Murphy, S. L. Cobb, *Org. Lett.* **2021**, *23*, 4672–4676.
[21] H. Meuzelaar, M. R. Panman, S. Woutersen, *Angew. Chem. Int. Ed.* **2015**, *54*, 15255–15259.
[22] a) C. J. White, A. K. Yudin, *Nat. Chem.* **2011**, *3*, 509–524; b) J. M. Humphrey, A. R. Chamberlin, *Chem. Rev.* **1997**, *97*, 2243–2266.
[23] M. Abbas, W. P. Lipinski, K. K. Nakashima, W. T. S. Huck, E. Spruijt, *Nat. Chem.* **2021**, *13*, 1046–1054.
[24] S. Cao, T. Ivanov, J. Heuer, C. T. J. Ferguson, K. Landfester, L. Caire da Silva, *Nat. Commun.* **2024**, *15*, 39.
[25] S. Kim, H. Y. Yoo, J. Huang, Y. Lee, S. Park, Y. Park, S. Jin, Y. M. Jung, H. Zeng, D. S. Hwang, Y. Jho, *ACS Nano* **2017**, *11*, 6764–6772.
[26] a) A. Baruch Leshem, S. Sloan-Dennison, T. Massarano, S. Ben-David, D. Graham, K. Faulds, H. E. Gottlieb, J. H. Chill, A. Lampel, *Nat. Commun.* **2023**, *14*, 421; b) D. Mandal, R. K. Tiwari, A. N. Shirazi, D. Oh, G. Ye, A. Banerjee, A. Yadav, K. Parang, *Soft Matter* **2013**, *9*.
[27] a) F. Späth, C. Donau, A. M. Bergmann, M. Kränzlein, C. V. Synatschke, B. Rieger, J. Boekhoven, *J. Am. Chem. Soc.* **2021**, *143*, 4782–4789; b) C. Donau, F. Späth, M. Stasi, A. M. Bergmann, J. Boekhoven, *Angew. Chem. Int. Ed.* **2022**, *61*, e202211905; c) A. M. Bergmann, J. Bauermann, G. Bartolucci, C. Donau, M. Stasi, A. L. Holtmannspötter, F. Julicher, C. A. Weber, J. Boekhoven, *Nat. Commun.* **2023**, *14*, 6552.
[28] N. Kolchina, V. Khavinson, N. Linkova, A. Yakimov, D. Baitin, A. Afanasyeva, M. Petukhov, *Nucleic Acids Res.* **2019**, *47*, 10553–10563.
[29] a) J. Schindelin, I. Arganda-Carreras, E. Frise, V. Kaynig, M. Longair, T. Pietzsch, S. Preibisch, C. Rueden, S. Saalfeld, B. Schmid, J. Y. Tinevez, D. J. White, V. Hartenstein, K. Eliceiri, P. Tomancak, A. Cardona, *Nat. Methods* **2012**, *9*, 676–682; b) X. Chen, H. Soria-Carrera, O. Zozulia, J. Boekhoven, *Chem. Sci.* **2023**, *14*, 12653–12660.

Manuscript received: April 18, 2024
Revised manuscript received: July 10, 2024
Accepted manuscript online: July 28, 2024
Version of record online: September 12, 2024

© 2024 The Author(s). Angewandte Chemie International Edition published by Wiley-VCH GmbH

15213773, 2024, 42, Downloaded from https://onlinelibrary.wiley.com/doi/10.1002/anie.202407424, Wiley Online Library on [14/11/2024]. See the Terms and Conditions (https://onlinelibrary.wiley.com/terms-and-conditions) on Wiley Online Library for rules of use; OA articles are governed by the applicable Creative Commons License